RSC Advances

ROYAL SOCIETY OF CHEMISTRY

www.rsc.org/advances

Triticale Crops Residue: A Cheap Material for High Performance Nanofibrillated Cellulose

Sami Boufi[a*], Alessandro Gandini[b]

[a] University of Sfax, Faculty of Science of Sfax, LMSE, BP 1171-3000 Sfax, Tunisia

[b:] The International School of Paper, Print Media and Biomaterials (Pagora), UMR CNRS 5518, BP 65, 38402 Saint Martind'Hères Cedex, France

** Corresponding author:*
Sami Boufi
University of Sfax-Faculty of science
BP 1171-3000 Sfax-Tunisia
Fax: 216 74 274 437
E-mail Sami.Boufi@fss.rnu.tn

Abstract

Nanofibrillated cellulose (NFC) from biomass has become a subject of intense research activities owing to the attributes of nanosized cellulose along with their sustainable character. However, efficient production of nanofibrillated cellulose is still challenging with respect to the energy required for the disintegration process. In this study, triticale crops residue was used as a source for the production of nanofibrillated cellulose, with lateral size of 20-30 nm, using a high pressure homogenizer and a conventional high speed blender. The effect of the delignification mode, the fibers pretreatment and the disintegration mode on the yield of NFC, the morphology of the ensuing nanofibrils and the energy consumption were investigated. The evolution of the reinforcing potential of the NFC according to the production mode was also studied. By controlling the lignin extraction mode and the carboxyl content of the fibers through TEMPO-mediated oxidation, it was possible to convert triticale pulps into nanofibrillar cellulose with energy demand as low as 11 KWh/kg using a conventional high speed blender. This approach is expected to open the way toward easier and energetically cost-effective production of nanofibrillar cellulose from crops residue.

Key words: nanofibrillated cellulose, triticale, crops residue.

Abbreviation

D1: NaOH delignification

D2: $NaClO_2$ delignification

O1: TEMPO mediated oxidation with $NaClO_2$ at pH 7

O2: TEMPO mediated oxidation with NaClO at pH 10-11

HPH: Disintegration using a high pressure homogenizer (10 passes at 600 Bar)

HSB: Disintegration using a high speed blender for 20 min

1. Introduction

Nanofibrillated cellulose (NFC) refers to nanosized cellulose fibrils formed by long, flexible and entangled cellulose nanofibrils and is composed of bundles of elementary fibrils (or cellulose microfibrils) separated by less-ordered regions. Depending on the plant species and the mode of preparation, the lateral dimensions of the nanofibrils are of the order of 10 to 100 nm with lengths in the micrometer scale. This class of natural nanofibrils constitutes a real breakthrough in cellulose-based materials and has become a topic of great interest in the last decade[1]. Their nanoscale dimensions, biodegradable character, cost effectiveness, high aspect ratio, light weight and sustainability constitute an impetus for this increasing interest. All of these attributes make nanosized cellulose very attractive for a broad range of applications within the field of innovative materials[2,3]. Furthermore, according to the current knowledge, nanocellulose is classified as a non-toxic material[4], completely biodegradable and without adverse effects on the health or the environment. These benefits facilitate the use of nanocellulose and eliminate safety concerns, commonly encountered, for mineral and carbon nanofillers.

Given its exceptional high stiffness and strength along with its high capacity to build up a rigid entangled network, NFC has gained considerable attention as one of the most promising reinforcements in the realm of sustainable nanofillers with a broad range of potential applications, such as for creating low-weight polymer-based composites[5,6,7] strength additives for paper[8,9,] barrier packagings[10] and adsorbent products[11].

NFC is produced by delaminating cellulosic fibers under an intense mechanical shearing action in order to break up the cell walls and release the nanosized fibrils. In addition to the high pressure homogenization (HPH) and micro-fluidization, which are the main methods currently used for the production of NFC, other means of generating microfibrils were

reported in the literature such as grinding and ultrasound-assisted fibrillation. However, irrespective of the disintegration process adopted, the production of NFC faces two major problems, namely (1) the clogging of the pulp, when the pulp is pumped through high pressure fluidizers/homogenizers, and (2) the high energy consumption needed for the efficient delamination of the cell wall via multiple passes through the homogenizer. This high-energy input is necessary in order to overcome the strong hydrogen interactions among neighbouring microfibrils. Values ranging from 20 to 50 KWh/Kg have been reported[12]. Therefore, one of the most important challenges associated with the production of NFCs on an industrial scale is to decrease the energy demand and facilitate the overall process. Pretreatment is sometimes used to address this problem. Enzymatic, mechanical or chemical pretreatment has shown to heavily decrease the energy demand[13]. This latter approach turned out to be one of the most efficient processes to facilitate the break up of the fibre network and release the microfibrils through an electrostatic repulsion and osmotic effect[14]. In this context, the TEMPO-mediated oxidation is the prevalent method to generate carboxylic groups in a controlled way. An obvious correlation between the carboxyl content and the ease of fibrillation was pointed out in several publications[15]. Furthermore, the chemical composition of the cellulose source, namely in terms of the hemicellulose content, was found to play a key role in the efficiency of the nanofibrillation process. The higher the hemicellulose content, the easier is the nanofibrillation aptitude of the fibres[16].

Although woody fibres remain the main source for the production of NFC, in practice, any resource of cellulose fibres could also be used. Specifically, agricultural crops and by-products, such as wheat straw, rice straw, rapeseed and corn stalks are the most abundant resources on earth and are an underutilized source of cellulose that are generally allowed to decompose in the fields or are burned for energy production. This class of biomass has received increasing attention in recent years as an alternative resource for the extraction of cellulose fibers. Several studies have been concerned with the extraction of NFC from agricultural crops[17,18,19] and all adopted a high consuming energy device, making NFC costly to produce. In comparison with wood, agricultural crops have shorter growth cycles, do not compete with the supply of wood and have a lower lignin content, making the delignification process easier. Triticale (*Triticosecale* Wittmack) which is a hybrid crop developed by crossing wheat (*triticum)* and rye (*secale)* is widely used as an industrial crop because of the higher yield in grain and biomass (straw), compared with the other cereal crops. As such, the utilization of triticale can increase the available biomass for industrial use without increasing competition with food production for agricultural land.

In the present work triticale straws were used as a starting material to produce NFC, adopting high-pressure homogenization and conventional high-speed blender for the disintegration process. The main emphasis is to highlight how the delignification process and the fibre activation can affect the ease of the nanofibrillation process. Particularly, it will be shown that under specific conditions of the delignification process and fibres pre-treatment, the nanofibrillation process can be implemented by simply using a conventional high-speed blender.

2. Experimental section

2.1 Samples

Triticale straws were harvested at maturity by the end of June. After further drying, the straws were ground to a coarse powder and crude fibres were Soxhlet extracted for 12 h , using first a solvent mixture composed of toluene/ethanol (60/40 v/v) and then hot water (70°C) for 1 h to remove pectin and sand.

The pulping procedure for the crude fibres was carried out as follows:

2.2.1 Delignification processes

Soda pulping procedure (designated here as D_1)

The extracted biomass was added to water (solid content 10 wt%) and then pulped with a 5 wt% NaOH solution for 2 h at 70-80 °C under mechanical stirring. This treatment was repeated three times until the fibres were well individualized. The ensuing fibres were subsequently filtered and rinsed with distilled water and twice bleached with $NaClO_2$ to remove the residual lignin.

$NaClO_2$/Acetic acid pulping procedure (designated here as D_2)

The $NaClO_2$/AA pulping process was carried out as follows: Five grams of dry soxhlet extracted biomass were added to water and mixed to form suspension at a solid content 10 wt%. Then, 0.5 g of sodium chlorite ($NaClO_2$) and 0.5 ml of acetic acid per gram of dry biomass were added, and the suspension was kept under mechanical stirring at a temperature of 70 °C for 6 h without removal of any liquor. Fresh charges of sodium chlorite and acetic acid were added to the reaction every 1.5 h for up to 6 h.

The pulp yield is calculated through equation 1:

$$\text{Pulp Yield } \% = \frac{\left[m_w(1 - MC/100\right]}{m_d} \times 100 \qquad (1)$$

where, m_w, m_d and MC are the weight of the wet biomass recovered, the weight of the dry sample used and MC the moisture content of the recovered solids, respectively.

2.2.2 Bleaching procedure

The bleaching treatment was carried out at 70 °C for 1 h at pH 4.8. The solution was composed of equal parts of aqueous chlorite (1.7 wt% $NaClO_2$ in water) and an acetate buffer (27 g NaOH and 75 mL glacial acetic acid diluted to 1 L of distilled water).

2.3 Chemical composition

The determination of the basic chemical composition was conducted following TAPPI standard protocols. (TAPPI T 257 cm-02). Samples were first submitted to Soxhlet extraction with ethanol/toluene and water. Then the chemical contents were determined using the following methods, Ash (Tappi T 211 om-93) extractive (Tappi T264 om-07), Klason lignin (Tappi T222 om-88), and hemicelluloses (Tappi T249-cm-85).

2.4 Fibre length measurements

Fibre length, width and curl index of the pulps and the length and width of the particles were measured by image analysis using a MorFi Lab equipment.

2.5 *TEMPO-mediated oxidation*

The TEMPO-mediated oxidation was carried out at pH 7 and 10, using $NaClO_2$ and NaClO as oxidizing agents, respectively. These two methods denominated TEMPO-NaClO-$NaClO_2$ and TEMPO-NaBr-NaClO were implemented, as described below:

*TEMPO-NaClO-$NaClO_2$ (O1): Cellulose fibres (2 g) were dispersed in a 0.05 M sodium phosphate buffer (200 mL, pH 7) solution, containing TEMPO (40 mg). Sodium chlorite and the 2 M (1.5 g) sodium hypochlorite solution 12° (4 mL) were added to the flask, which was stppered and stirred at 500 rpm and 60 °C for 12 h. The oxidation was stopped by adding 50 mL of ethanol, and the oxidized fibres were filtered and washed twice using deionised water.

*TEMPO-NaBr-NaClO (O2): Cellulose fibres (2 g) were suspended in 200 mL water. TEMPO (30 mg) and NaBr (250 mg) were added to the suspension. Then 50 mL of a

commercial NaClO solution (12°) was added dropwise to the cellulose suspension at a temperature around 5°C, kept constant throughout the oxidation reaction. The pH was maintained around 10 by the continuous addition of a 0.1 M aqueous solution of NaOH. The oxidation was stopped by adding ethanol (20 mL) and the pH was adjusted to 7 by adding 0.1 M HCl.

2.6 Carboxyl content

The carboxyl content of the oxidised cellulose was determined using conductimetric titration, as described elsewhere[14].

2.7 Fibrillation process

High pressure homogenization (HPH): NFC was prepared from the delignified pulp by pumping through a GEA Homogenizer processor (NS1001L PANDA 2 K-GEA, Italy). The homogenization was conducted in two steps. Firstly, the fibre suspension at a concentration of 1.5 wt% was passed several times through thin slits at a pressure of 300 bar (4350 Psi) until the suspension turned to a gel. Then, the fibrillation was pursued by further passes at a pressure of 600 bar (8700 Psi).

Fibrillation using a conventional high speed blender (HSB): the fibres in a water suspension at a concentration of 2 wt% were disintegrated during 15-20 min in a "one-step operation" using a domestic high speed blender (MOULINEX 400 W) with a constant running speed of 11 000 rpm, in which the blades rotate in a recessed section at the bottom of a container of 1 L capacity.

2.8 Yield in nanofibrillated cellulose

Centrifugation of a diluted NFC suspension was shown to be an efficient means to separate the unfibrillated materials[14] from those partially fibrillated. The protocol was carried out as follows: a dilute suspension with about 0.1 wt% solid content (Sc) was centrifuged at 4500 rpm for 20 min to separate the nanofibrillated material (in supernatant fraction) from the non-fibrillated or partially fibrillated ones, which settle down. Then, the sediment fraction was dried to a constant weight at 90 °C. The yield was calculated from Eq.2

$$Yield\ \% = \left(1 - \frac{\text{weight of dried sediment}}{(\text{weight of diluted sample} \times \%\text{Sc})}\right) \times 100 \qquad (2)$$

The results represented the average values of three replications.

2.9 Field-emission scanning electron microscopy (FE-SEM)

A Weiss SEM was used to obtain images by capturing secondary electrons emitted from the surface of a NFC sample, prepared from a drop of the NFC suspension (with a solid content about 0.05 wt%) deposited on the surface of a silicon wafer and coated with a thin carbon layer, applied by ion sputtering with a thickness limited to 2 to 3 nm. To ensure a good image resolution without any damage to the samples during the analysis, the acceleration voltage was maintained at a relatively low range (2-5 kV).

2.10 Determination of the crystalline index

The crystallinity was evaluated from an X-ray diffraction (XRD) pattern obtained using a BRUKER AXS diffractometer (Madison, WI) with a Cu-K_α radiation, generated at 30 kV and an incident current of 100 mA. The (2θ) angular region from 5° to 40° was scanned by steps of 0.05° using a step time of 10 s. The crystalline index (CrI) was calculated by equation 3 using the diffraction intensities of the crystalline structure and that of the amorphous fraction, according to the method of Segal et al[20]:

$$CrI\% = \left[\frac{I_{002} - I_{am}}{I_{002}}\right] \times 100 \qquad (3)$$

where I_{002} is the maximum intensity of the (002) diffraction peak, taken at 2θ between 22° and 23° for cellulose I, and I_{am} is the intensity of the amorphous diffraction peak taken at 2θ between 18° and 19° for cellulose I.

Scherrer's equation was used to calculate the crystallite size, T (nm), perpendicular to the (200) plane for cellulose I crystals:

$$T = \frac{K\lambda}{\beta.\cos\theta} \qquad (4)$$

Where K is a dimensionless shape factor and usually taken to be 0.9, λ (1.54 Å) is the X-ray wavelength, β is the line broadening at half the maximum intensity (FWHM), in radians, and θ is the diffraction angle

2.11 Energy consumption

The instrument used for the energy consumption measurement was a power analyser from SCOMEC DIRIS A20 which is an integrating tool that measures precisely the total amount of

electrical energy, the voltage and the current intensity supplied to the electrical equipment in a given period of time.

2.12. Nanocomposites processing

Commercial acrylic latex obtained by the copolymerization of styrene (S) and butyl acrylate (BuA) was used as a matrix. The size of the polymer particles was around 150 nm and the solid content 50 wt%. The glass–rubber transition temperature (Tg) of this poly(S-co-BuA) copolymer was about -10°C.

The NFC gel was mixed with the latex in order to obtain nanocomposite films with weight fraction of cellulose ranging from 0% to 15%. After stirring for 1h, the mixture was cast in a Teflon mould and stored at 40°C until water evaporation was completed. A transparent to translucent film, depending on the NFC content, was obtained with a thickness in the range of 300 to 400 µm.

2.13. Tensile tests

The non-linear mechanical behaviour of the films was analyzed using an Instron testing machine in tensile mode, with a load cell of 100 N working at a strain rate of 10 mm/min at 25 °C . The specimens were obtained using a cutting device.

2.14. Transparency measurement

The transparency of neat acrylic film and nanocomposite films was measured at wavelengths from 200 to 800 nm using a UV-visible spectrometer (Lambda 35, Perkin-Elmer). The transmission spectra of the films were recorded using air as reference.

The following abbreviations were used to design the different means of treatment performed during the production of NFC:

3. Results and discussion

3.1 Pulp characterization

The typical feature of the stem anatomy was analyzed by SEM observation of transverse sections of the stem. As shown in Figure 1, several different cell elements, namely parenchyma, vascular tissue, epidermis, and the fibre cells can be perceived. These micro-structural aspects are related to different functions in the plant. The parenchyma cell acts as

carbohydrate storage, the vascular tissues provide long distance transport and the structural support and elementary fibres inside the fibre bundles supply the mechanical support. Most of the fibres displayed a large lumen width, in the range of 10 to 20 µm and the thickness of the cell walls layed between 2 to 5 µm, depending on their position in the stalk, the outer cells being thicker than the inner ones.

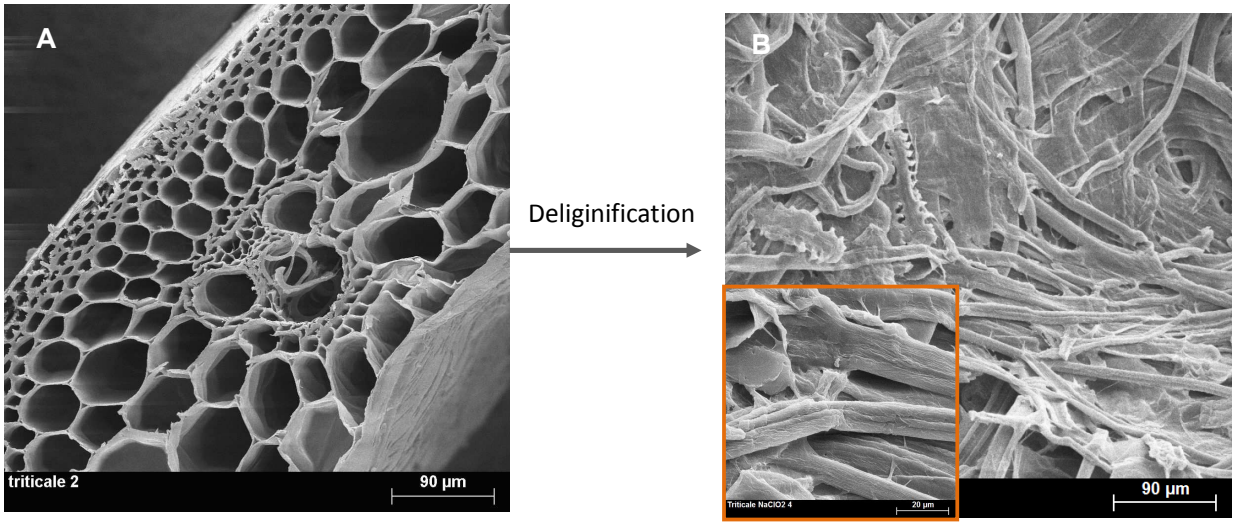

Figure 1 : SEM observation of (1) cross-section of triaticale straw, and (B) of the ensuing fibres after the deliginification process.

Given the lower lignin content in the crops residues, along with their more open structure compared to those of hard- and softwoods, milder pulping conditions with no sulfur processes can be applied for the lignin extraction.

The chemical composition of native triticale straw, NaOH and $NaClO_2$ extracted fibres are given in Table 1. Native triticale was composed of 39, 31, 21 and 5 cellulose, hemicelluloses, lignin and ash, respectively. This composition is typical of agricultural crops residue[21]. Ash was mainly composed of silica, as confirmed by XRD (Figure 2). $NaClO_2$ deliginification led to the effective removal of lignin, with the highest yield around 65 %. The ensuing pulp was white, without any necessity to implement a bleaching treatment. By means of the soda pulping process, a brown pulp was obtained with a yield of around 45 %. The specificity of each deliginification method accounts for the pulp characteristics. Actually, contrary to the soda pulping method known to remove lignin as well as a high fraction of hemicelluloses, the

271 $NaClO_2$ method is more selective for lignin[22] and preserves most of the hemicelluloses in the
272 biomass[23].

273 **Table 1.** Chemical composition (wt %) and properties of the agricultural by-products used here.

Constituents	Native triticale straw	NaOH extracted	NaClO2 extracted
Cellulose	39±1	84±2	71±2
Hemicellulose	31±1	16±1	29±1
Lignin	21±1	-	-
Ash	5±0.5	-	-
Hot water extractible	4		
	Properties		
Pulp yield	-	45±3	65±3
Fibres length (μm)	-	840±50	700±50
Fibres width (μm)	-	22±4	21±4
CrI	48±2	60±2	74±2

274 ** Solubility in hot water in %*

275 *** as % of dry matter.*

276

277 The peaks at 2θ values of 15.2º, 16.7º, and 23.1º corresponding to (101), $(10\bar{1})$, (002)
278 planes, respectively, are the diffraction peaks of ellulose I structure (JCPDS. No. 03-0226).

279 The XRD characterization revealed the presence of the main characteristic peaks of cellulose I
280 (JCPDS. No. 03-0226) at 2θ values of 15.2º, 16.7º, and 23.1º corresponding to (101), $(10\bar{1})$,
281 (002) planes, respectively, for all studied samples, before and after the extraction procedure,
282 indicating the preservation of the native crystalline structure even in the presence of the NaOH
283 treatment. After the lignin extraction, the crystallinity index increased due to the partial
284 removal of the amorphous hemicelluloses and lignin. In addition, lower crystallinity indexes
285 were found when the lignin extraction was implemented with the $NaClO_2$ procedure, which is
286 in accordance with the highest content of hemicellulose in these samples. The XRD revealed
287 the presence of silica (SiO_2) (JCPDS. No. 33-116) on the triticale straw, which was completely

removed after the deliginification treatment. This presence accounts for the relatively high ash content of triticale compared to woody plants. The presence of silica is typical of agricultural crops residue. It is accumulated in the form of SiO_2 by transport of water-soluble silicic acid from the soil to the plant tissues through the roots. This element is of significance in the life of plants and the performance of crops. During the sclerification of the cell wall, $Si(OH)_4$ undergoes condensation to give the Si-O-Si oligomers that further grow to form SiO_2 nanoparticles. Silicic acid also acted as a cross-linking agent between the lignin and the carbohydrate[24], via complexations with phenolic acids and the hydroxyl groups of hemicelluloses and cellulose.

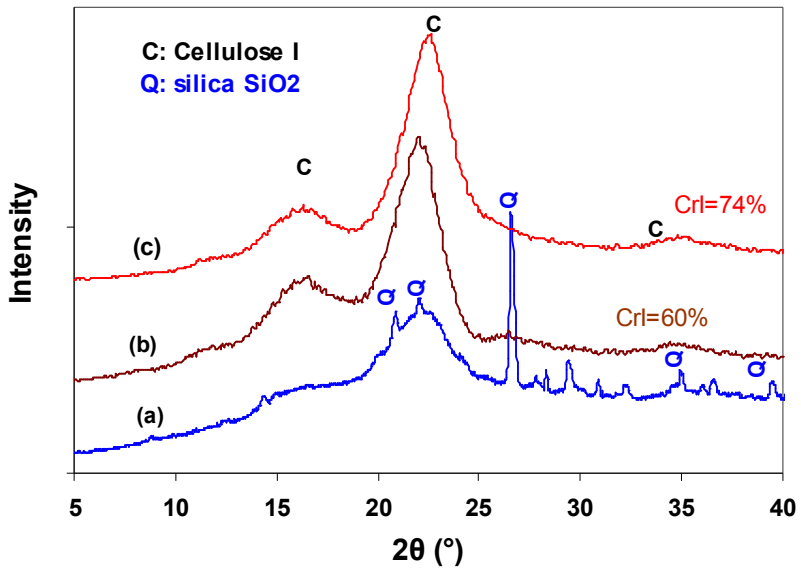

Figure 2 : XRD patterns for (a) neat triticale straw, (b) NaOH delignified, and (c) $NaClO_2$ delignified pulps.

The morphology of the fibres extracted from the crop residues exhibited typical cells already observed in the cross-section of the stems (Figure 1B). In addition to the fibres, other non-fibrous cell elements, such as vessels and parenchyma cells, could be distinguished. The fibrous cells were collapsed to approximately 10-30 µm in width and characterized by thin cell walls about 2-5 µm thick. The vessels and collenchyma cells were larger than other cells, with a rectangular shape approximately 100–300 µm long and 40–50 µm wide. The mean length

and width of the delignified fibres, determined from MORPHI analysis, were around 500-600 μm and 20 μm, respectively.

3.2 Nanofibrillation behaviour of the fibres

A high-pressure homogenizer (HPH) and a high-speed blender (HSB) were used as mechanical devices to breakup the cell wall and release the cellulose microfibrils. The former process is the conventional approach commonly adopted to produce NFC, but with a high-energy input. The latter was employed here as a low energy demand method to produce NFC. For both approaches, the fibres were first submitted to a TEMPO-mediated oxidation pre-treatment to bring the carboxyl content up to 500 μmol/g and to facilitate the defibrillation process. The oxidation pretreatment aims at generating carboxylic groups, whose ionization facilitates the fibrillation and the break-down of the cell wall of the fibres through different effects, namely: (a) the oxidation generates negative charges that bring forth repulsive forces between microfibrils within the cell wall; (b) the oxidation favours the hydration and swelling of the fibres, making them more flexible; (c) the oxidation loosens the primary and S1 cell walls, making the S2 layer more accessible and more prone to fibrillation during the homogenization process; and finally (d), the oxidation results in chain scission in the amorphous zones, creating defaults within the fibre cell wall, which facilitates the mechanical fibrillation.

The oxidation was carried out either at neutral or basic pH (viz. the O1 and O2 modes) using $NaClO_2$ and NaClO as oxidizing agents, respectively. Although both methods are specific to the selective oxidation of the C6 primary alcohol groups into aldehydes and/or carboxylic acid groups, they affect differently the degree of polymerization[25] (DP) of the oxidized cellulose. The former (O1) led to a significant decrease of more a factor of five, whereas the latter left essentially unchanged.

To clearly distinct between the different NFC samples, a chart diagram showing all the steps adopted to generate NFC from triticale straw, with their corresponding abbreviations is given in scheme 1.

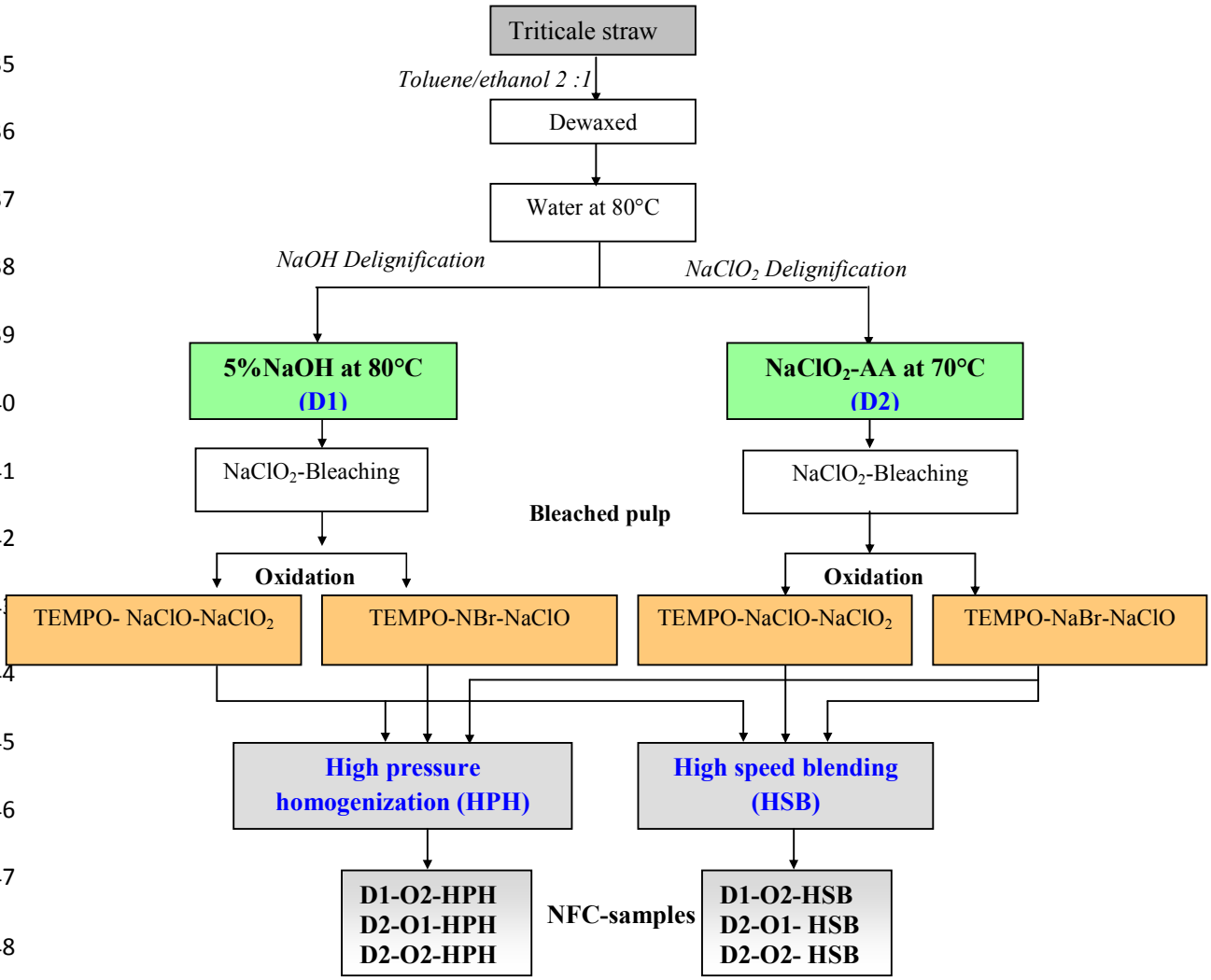

***Scheme 1**: Illustrative scheme of the various treatments performed on the triticale straw for the preparation of NFC samples by a high pressure homogenization (HPH) and a high speed blender (HSB).*

The change in the fibrillation yield and in the transparency degree at 700 nm according to the pulping mode, the oxidation method and the disintegration mode are given in Figure 3. The highest fibrillation yield, exceeding 95%, was achieved using HPH starting from fibres delignified via $NaClO_2$ (D2-O2-HPH and D2-O1-HPH). This means that when a high content in hemicelluloses was left in the fibers after the deliginification and bleaching treatments, the fibers were effectively fibrillated into NFC via HPH, irrespective of the oxidation mode. However, a slightly higher transparency degree of the NFC gel was observed when the O2oxidation route was adopted (Transparency close to 94% for the O2 oxidation against 84% for O1). However, a decrease in the fibrillation yield as well as in the transparency were noted

when NaOH deliginified mode was used, even when the HPH disintegration mode was adopted. Interestingly, when lignin extraction was performed via $NaClO_2$ mode, it was possible to disintegrate cellulose fibers into NFC using a conventional HSB. Both of the two oxidation routes (O2 or O1) led to a high fibrillation yield (around 88%) and good transparency (samples D2-O2-HSB; D2-O1-HSB). On the other hand, when the deliginification was carried out with NaOH, a translucent NFC gel was obtained with a fibrillation yield that do not exceed 50% fibrillation yield, even after prolonged disintegration in the HSB for more than 30 min for (sample, D1-O2-HSB). The fibrillation yield further decrease to about 20% when the NaOH delignified fibers were oxidized via O1 route (D1-O1-HSB). This means that fibers became hard to be converted into NFC via the HSB when the lignin extraction was performed with NaOH, especially when the TEMPO-mediated oxidation was carried out at neutral pH (O1 route).

The easier fibrillation ability of $NaClO_2$ deliginified fibres is explained by the higher residual hemicelluloses content left in the fibres that contributed to reduce the interaction via hydrogen bonding among cellulose microfibrils within the cell wall. The key role of hemicelluloses in the fibrillation process has been highlighted in our previous work[26]. Thanks to their amorphous and highly hydrated character, the hemicelluloses surrounding the microfibrils behave as a protective colloid preventing the microfibrils from coming close together to self-associate into larger aggregates through hydrogen bonding. A schematic view of the assembly mode of cellulose microfibrils according to the delignification route is given in Scheme2.

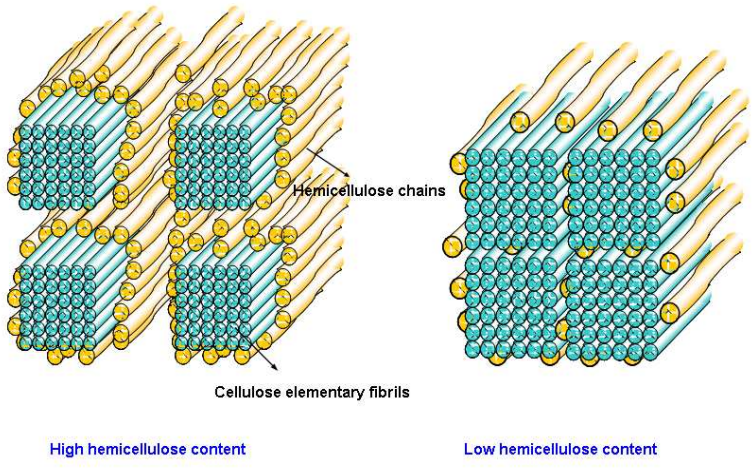

Scheme 2: *Schematic illustration of the microfibrils assembly according to the content of hemicellulose within the fibers*

The low cell wall thickness of triticale fibres is another reason likely to facilitate the break-up of the cell wall via HSB mechanical disintegration.

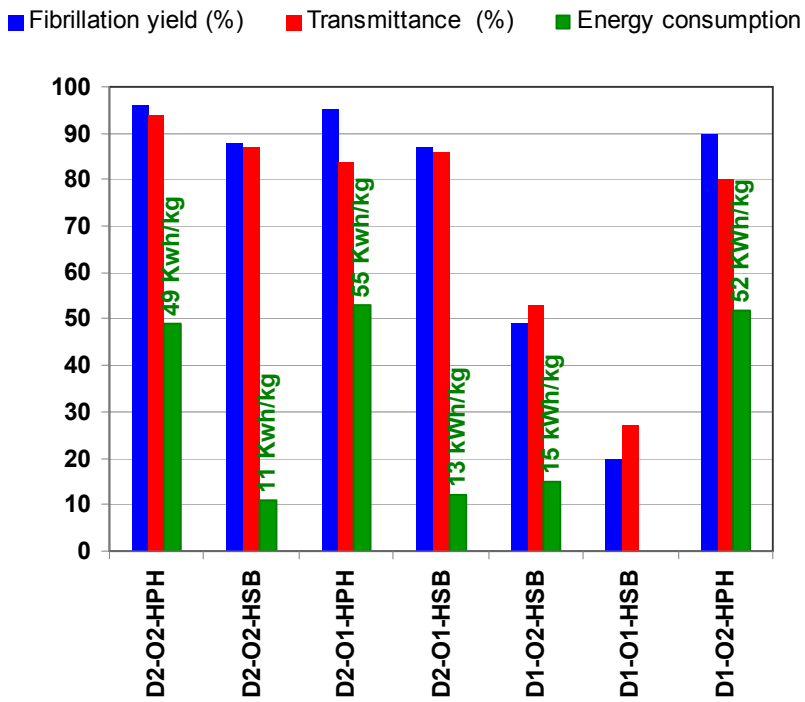

Figure 3: Evolution of the fibrillation yield, transmittance of the NFC gel and energy consumption (per Kg of dry NFC) during the production of NFC following the different routes adopted in this study.

The difference in the optical aspect of the NFC gel was further highlighted from the digital photos showing the aspect of the NFC gel produced from triticale via the methods discussed above (Figure 4). The most transparent NFC suspensions were those where the delignification was implemented using D2 ($NaClO_2$/acetic acid) process. Both of the HPH and the high speed blender (HSB) modes of disintegration led to NFC suspensions with a higher transparency level, which is indicative of highly nanofibrillated cellulose. In contrast, the NaOH delignification (D1) mode led to an opaque NFC suspension, namely when HPB was used for the disintegration (D1-O2-HSB). The difference in the optical transparency of the NFC gel is essentially due to the difference in the nanofibrillation extent of the fibers. The presence of

399 partially fibrillated materials with a width larger than 100 nm led inevitably to a huge drop in
400 the transparency of the NFC gel because of light scattering at water-fibrils discontinuity.

401

402

403

404 **Figure 4:** visual aspect of NFC from triticale at a solid content of 1wt%, according to the
405 production mode.

406

407

408 Although the energetic input during the nanofibrillation process is a key issue in the
409 cost production of NFC, the quantification of energy input according to the fibers
410 preatreatment has been reported only in a few papers [27,28]. In addition, it is important to keep
411 in mind that energy consumption should be defined with respect to a given degree of
412 fibrillation or a set value of gel-transparency. This is an important point, since the change
413 from a liquid to a gel-like form of the fibers suspension did not imply the conversion of the
414 whole cellulose fibers into nanofibrillated material. A nanofibrillation extent of over 90%
415 requires necessarily a high-energy input to completely breakup the cell wall and release the
416 cellulose microfibrils or bundles of cellulose microfibrils. The energy consumption for the
417 different approach adopted in the present work was also included in Figure 3. Starting from
418 $NaClO_2$/AA delignified fibres, the energy input necessary to attain a fibrillation yield of
419 around 90% was in the range of 40-45 kWh/kg of dry NFC with HPH and decreased to about
420 9-12 kWh/kg when HSB was used. This corresponds to a 80% reduction in energy input. The
421 need to raise the pressure up to 500-700 bars during the HPH processing is the origin of the
422 high energy consumption of this disintegration mode.

423

424 **3.3 Morphology of NFC**

425

426 The morphology of the different samples of NFC prepared via different approaches
427 was analysed using FE-SEM, performed on the supernatant fraction (Figure 5). NFC
428 obtained by the (D2-O1-HPH) and (D2-O1-HSB) routes were composed of individualized
429 fibrils with a width of 20-30 nm and a length exceeding 2 µm. If one takes into account the
430 coating metallisation layer necessary for FE-SEM observation to be within a 2-3 nm

thickness, then the ultimate width should be in the range of 15-20 nm and the aspect ratio exceed 100. It turns out that the width of the NFC was much higher than the average thickness of cellulose crystallites which is around 3.5 nm, as calculated according to the Scherrer equation. This means that the ensuing nanofibrils were, in turn, formed by bundles of elementary cellulose fibrils, regardless of whether HPH or HSB were used for the disintegration process.

NFC produced via (D2-O2-HSB) or (D2-O2-HPH) exhibited quite the same width, but looked shorter than those produced via (D2-O1-HSB) or (D2-O1-HPH). Their length was lower than 1 µm, which led to an aspect ratio of about 50. The difference in the NFC length according to the oxidation mode (neutral vs basic pH) was explained by the higher extent of the degree of polymerization reduction when the oxidation was carried out under basic conditions. Indeed, it was reported that the TEMPO-NaBr-NaClO at pH 10 led to a remarkable cleavage of polysaccharides as a result of the β-elimination promoted by the presence of C6-aldehydes formed as an intermediate structure, and through a radical scission resulting from the formation of hydroxyl radicals during the oxidation process[29]. The decrease in the degree of polymerization during the oxidation process led inevitably to a fall in the length of the cellulose microfibrils. This correlation can be understood if one assumes that during the oxidation process, the amorphous domains are more prone to oxidation than the crystallite domains, due to their higher accessibility. Given the ultratsructure of the microfibrils being composed of alternating crystallite and disordered amorphous domains regularly distributed along the microfibrils axis, the resulting breakup in the chains within the amorphous domains led inevitably to a shortening in the microfibrils length. Similar results were reported by Benhamou et al[30] revealing a reduction in the fibrils length, as the carboxyl content increased and the oxidation was carried out at basic pH.

NFC produced from NaOH-delignified pulps by HSB (D1-O2-HSB) showed in addition to the nanosized thin fibrils with width lower than 20 nm, not fully disintegrated macrofibrils with a width in the range of 100-200 nm. Presumably, energy generated with the HSB process was not sufficient to completely breakup the hydrogen-bonding network holding the cellulose microfibrils. We infer that the remval of a high fraction of hemicelluloses during the pulping process with NaOH, brought the microfibrils into closer contact, making intermolecular hydrogen bonding more cohesive.

Figure 5: *FE-SEM images of NFC produced from tritical straw via high pressure homogenization and high speed blender.*

3.4. Reinforcing potential of NFC

To investigate the reinforcing potential of NFC from triticale produced by the different approaches, nanocomposite films were prepared via solvent-casting and tested using non-linear tensile tests performed at room temperature. A ductile water-borne acrylic matrix with a Tg around -10°C was chosen as a matrix in order to reach the limit strength without premature breaking of the sample due to excessive rigidity. Typical stress-strain curves obtained from tensile tests for NFC-based nanocomposite films are shown in Figure 6.The addition of NFC led to the steady enhancement in the tensile modulus as well as in the tensile strength. However, as shown in Figure 7, the increment was dependent on the preparation route of NFC. The highest reinforcing potential was associated with D2-O1-HPH ($NaClO_2$ delignification, oxidation at pH 7 and disintegration via HPH), followed by D2-O2-HPH, D2-O1-HSB and D2-O2-HSB. For instance, at 10 wt% NFC content, the respective increment in the tensile modulus/tensile strength were 160/27, 79/11, 70/11, and 22 time/5 time that of the neat matrix.

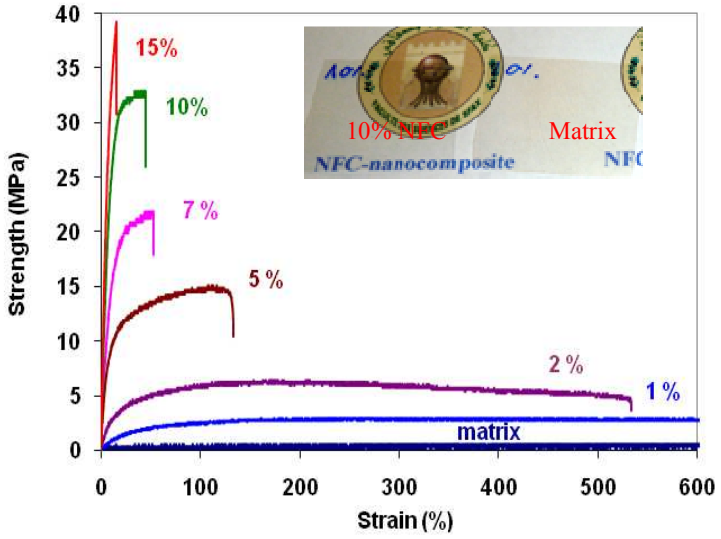

Figure 6: Typical stress–strain curves for nanocomposite films prepared from NFC produced via D2-O1-HPH

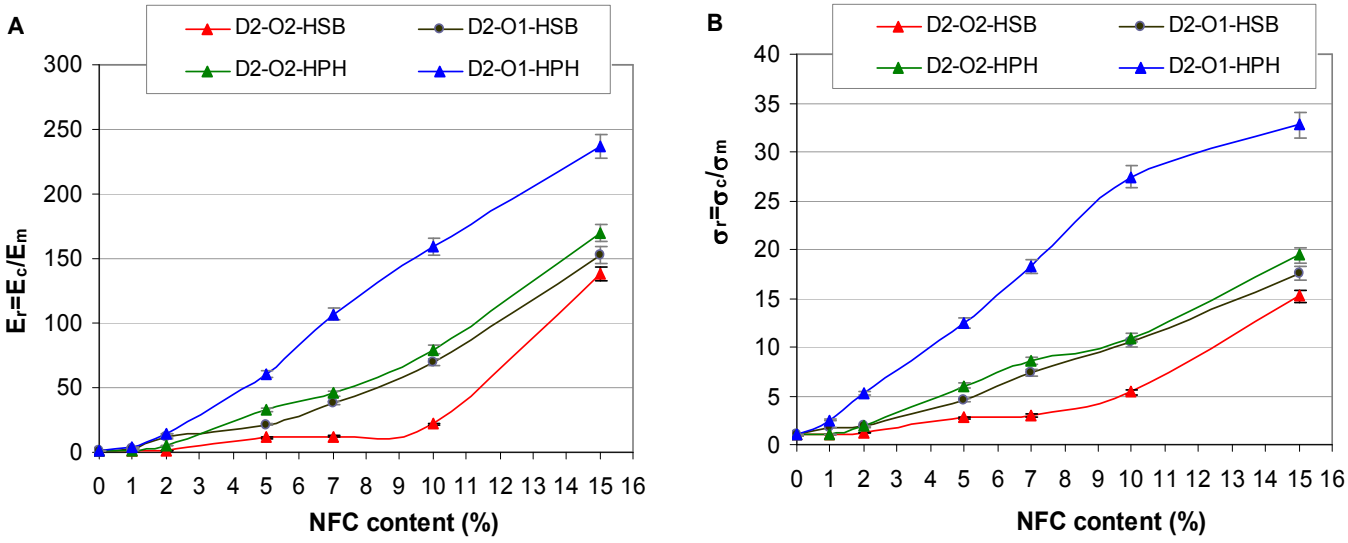

Figure 7: increment in (A) the tensile modulus, and (B) the tensile strength of nanocomposite films according to the NFC content and the mode of their production.

The stronger reinforcing potential of NFC produced by the D2-O1-HPH approach was attributed to the consequence of the higher length of the cellulose nanofibrils, as confirmed by the FE-SEM observations. The higher length, along with the narrow thin width of the NFC (about 20 nm as shown in Fig 5) produced through this approach, led to a higher aspect ratio that is more favourable to generate an entangled network. The set-up of an interconnected network held-up by strong hydrogen bonding is known to be a prerequisite in order to take advantage of the unusual enhancement of the stiffness and strength in the nanocellulose reinforced nanocomposites[31]. The concept of percolation originally adopted for rod-like cellulose nanocrystals was shown to be valid for NFC[5]. Accordingly, the tensile modulus of the nanocomposite is simply the product of the modulus of percolating filler network and thevolume fraction of the percolating filler phase (equation 5)

$$E_c = \psi E_r \qquad \textbf{(5)}$$

Where ψ can be written as:

$$\psi = 0 \qquad \text{For} \quad \phi < \phi_p \qquad (6)$$

$$\psi = \phi.\left(\frac{\phi - \phi_p}{1 - \phi_p}\right)^b \qquad \text{For } \phi \geq \phi_p \qquad (7)$$

Where ψ, ϕ and b are the volume fraction of the percolating network, the total volume fraction of the nanofiller and the critical exponent, respectively. Since the percolation threshold is inversely proportional to the aspect ratio of the dispersed objects, the higher the aspect ratio, the stronger is the reinforcing potential of NFC .

Interestingly, it can be seen that NFC produced via HSB (D2-O1-HSB) exhibited nearly the same reinforcing potential than that prepared via HPH (D2-O2-H) over the whole range of NFC loading. Here again, the higher aspect ratio of NFC from the (D2-O1-HSB) process compared to that from the (D2-O2-HPH) counterpart, accounts for the upholding of the reinforcing efficiency of the NFC, even though a high-speed blender was used for the disintegration process. This result is important to highlight since the production of NFC using a conventional high speed blender instead of the high pressure homogenizer or microfluidizer usefully adopted, contributed to make easier the scale-up production of NFC not only in term of plant facility but also on the basis of the energy cost. The drop in the reinforcing potential for NFC produced through (D2-O1-HSB) was likely due to its lower aspect ratio and lower fibrillation yield.

3.5. Optical Properties of the Nanocomposite Films

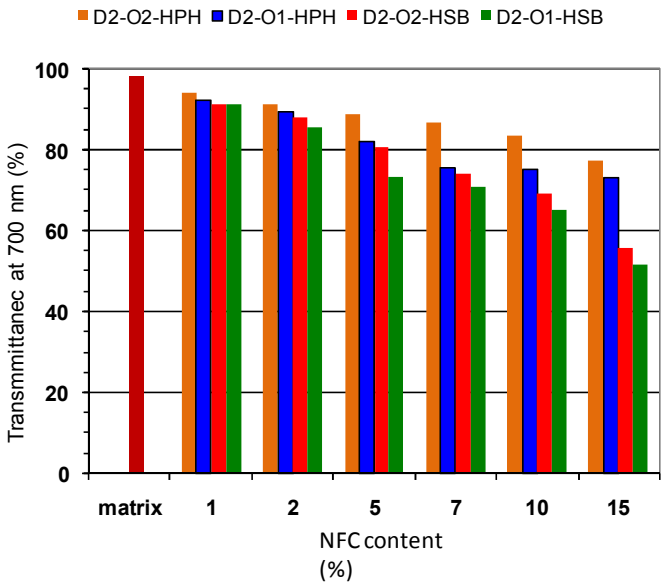

Figure 7. (a) Transmittance at 700 nm of nanocomposite film vs NFC content and according to their production mode.

Generally, in addition to the mechanical reinforcing effect provided by the inclusion of cellulose-based nanofiller in a polymer matrix, the optical transparency of the polymeric matrix is another aspect which is often aimed to be preserved. In general, for nanocomposite materials, the reduction in the transparency is caused by light scattering against the randomly dispersed particles, brought about by the discontinuity between the refractive index of the matrix and that of the nanofiller. The critical factor controlling the transparency of nanocomposites is the width of the nanofiller or, more specifically, the effective scattering cross-sectional area and its dispersion level within the host polymer matrix. In order to evaluate the optical transparency of the nanocomposites for different nanoparticle contents, the transmittance at 700 nm was used, and the results are shown in Figure 7a. The film transmittance was normalized to a 200 μm-thickness using the Beer–Lambert law, in order to avoid the effect of a small fluctuation in the film thickness. The addition of NFC led to a steady drop in the transparency of the film, namely over 7% NFC loading, where a ~20% decrease in the transmittance was noted. However, the decrease in the transparency depended on the NFC origin and the following order was noted D2-O2-HPH>D2-O1-HPH>D2-O2-HSB>D2-O1-HSB. The highest transparency was observed for nanocomposites with NFC produced via HPH, which was probably the consequence of a more effective fibrillation

degree brought about by the HPH. In fact, since the scattering intensity is proportional to the third power of particle size, the presence of partially fibrillated material with a size within the micron scale, even in a low proportion, led inevitably to a fall in transparency. However, it is interesting to note that over the whole range of NFC contents, a higher transmittance was noted for NFC from D2-O2-H, compared to that from D2-O1-HPH. This means that a longer NFC induced more scattering than a shorter one. The same trend was noted for NFC produced via HSB (D2-O2-HSB>D2-O1-HSB). This behavior is attributed to the higher tendency of longer cellulose nanofibrils to generate a bonded area through entanglement and cross-section contact with a higher thickness, once the water was removed and a film formed. The resulting bonded area brought therefore more scattering than individual nanofibrils.

4.Conclusion

Nanofibrillated cellulose from tritical straw was produced using both a high pressure homogenization and a conventional high speed blender. Alkaline and NaClO2/acetic acid pulping process was adopted to remove lignin and a TEMPO-mediated oxidation at two pH was carried out to bring the carboxyl content up to 500 µmol/g and facilitated the fibrillation process.

The delignification mode and the oxidation route were shown to control the fibrillation extent and the energy consumption during the disintegration process. The highest energy consumption was noted when the alkaline pulping process was adopted. The content of the residual hemicellulose left within the cellulose fibers after lignin removal was considered as key parameters controlling the fibrillation process and the energy consumption. The transparency degree of the NFC gel and the morphology of the cellulose nanofibrils were also dependent of the delignification and the disintegration mode. When the NaClO2/acetic acid pulping process and TEMPO-oxidation at neutral pH were implemented, long individual nanofibrils with width around 20 nm and length exceeding several µm were obtained via the high pressure homogenization as well as the high speed blender. The oxidation at basic pH led to a shorter nanofibrils resulting from the DP reduction during this chemical pretreatment. The change in the nanofibrils morphology according to the delignification/disintegration modes affected equally the reinforcing potential of the NFC. NFC produced from NaClO2/acetic acid delignified pulp using high pressure homogenization exhibited a reinforcing potential about two folds higher than that produced from high speed blender.

References

582

[1] Zhang1, Y.; Nypelö1 T.; Salas1 C.; Arboleda1 J.;. Hoeger1 I C.; Rojas O J.; Cellulose Nanofi brils: From Strong Materials to Bioactive Surfaces, J. Renew. Mater. **2013**, 1, 3, 195-211

[2] Kalia S.; Boufi S.; Celli A.; Kango S.; Nanofibrillated cellulose: surface modification and potential applications. Colloid. Polym. Sci. 2014, 292:5–31

[3] Abdul Khalil H.P.S.; Davoudpour Y.; Nazrul Islama Md.; Mustapha A.; Sudeshd K.; Dungania R.; Jawaid M. Production and modification of nanofibrillated cellulose using various mechanical processes: A review, Carbohydrate Polymers 99 (2014) 649– 665.

[4] Vartiainen J.; Pöhler T.; Sirola S.; Pylkkänen L.; Alenius H.; Hokkanen J.; Tapper U.; Lahtinen P.; Kapanen A.; Putkisto K.; Hiekkataipale P.; Eronen P.; Ruokolainen J.; Laukkanen A. Health and environmental safety aspects of friction grinding and spray drying of microfibrillated cellulose. Cellulose 2011,18, 775-786.

[5] Boufi S.; Kaddami H.; Dufresne A. Mechanical performance and transparency of nanocellulose reinforced polymer nanocomposites. Macromol. Mater. Eng. 2014, 299, 560–568

[6] Chaker A.; Mutje P.; Vilaseca F.; Boufi S. Reinforcing potential of nanofibrillated cellulose from nonwoody plants. Polym. Compos. 2014, 34, 1999-2007.

[7] Besbes I.; Rei Vilar M.; Boufi S. Nanofibrillated cellulose from alfa, eucalyptus and pine fibres: preparation, characteristics and reinforcing potential. Carbohyd. Polym. 2011, 86, 1198-1206.

[8] González I.; Boufi S.; Pèlach M. A.; Alcalà M.; Vilaseca F.; Mutjé P. Nanofibrillated cellulose as paper additive in bleached hardwood pulps. Bioresources 2012, 7, 5167-5180.

[9] González I.; Vilaseca F.; Alcalá M.; Pèlach M.; Boufi S.; Mutjé P. Effect of the combination of biobeating and NFC on the physico-mechanical properties of paper. Cellulose, 2013, 20 (3), 1425-1435.

[10] Lavoine N.; Desloges I.; Dufresne A.; Bras J. Microfibrillated cellulose – Its barrier properties and applications in cellulosic materials: A review, Carbohyd. Polym. 2012, 90, 735– 764

[11] Maatar W.; Alila S.; Boufi S. Cellulose based organogel as an adsorbent for dissolved organic compounds. Ind Crop Prod
2013, 49:33–42

[12] Klemm D.; Kramer F.; Moritz S.; Lindstrom T.; Ankerfors M.; Gray, D.; Dorris A. . Nanocelluloses: A new family of nature-based materials. Angew. Chem. Int. 2011,50, 5438-5466.

[13] Spence K. L.; Venditti R. A.; Rojas O. J.; Habibi Y.; Pawlak J.J.; A comparative study of energy consumption and physical properties of microfibrillated cellulose produced by different processing methods, Cellulose 2011,18, 1097–1111

[14] Saito T.; Nishiyama Y.; Putaux JL.; Vignon M.; Isogai A. Homogeneous suspensions of individualized microfibrils from TEMPO-catalyzed oxidation of native cellulose. Biomacromolecules 2006,7,1687–1691

[15] Besbes I.; Alila S.; Boufi S. Nanofibrillated cellulose from TEMPO-oxidized eucalyptus fibres: Effect of the carboxyl content. Carbohyd. Polym. 2011,84, 975-983.

[16] Chaker A.; Alila S.; Mutjé P.; Rei Vilar M.; Boufi S.. Effect of the Hemicellulose Content on the Nanofibrillation behaviour of Cellulose Pulps. Cellulose, 2013,20,2863-2875.

[17] Hassan M.L.; Mathew A.P.; Hassan E.A.; El-Wakil N.A.; Oksman K. Nanofibres from bagasse and rice straw: process optimization and properties. Wood Sci. Technol. 2012, 46, 193-205.

[18] Puangsin B.; Fujisawa S.; Kuramae R.; Saito T.; Isogai A. TEMPO-Mediated Oxidation of Hemp Bast Holocellulose to Prepare Cellulose Nanofibrils Dispersed in Water, J Polym Environ. 2013, 21:555–563

[19] Alila S.; Besbes I.; Rei Vilar M.; Mutj P.; Boufi S. Non-woody plants as raw materials for production of microfibrillated cellulose (MFC): A comparative study. Ind. Crop. Prod. 2013. 41, 250-259.

[20] Segal L, Creely JJ, Martin AE, Conrad CM. An empirical method for estimating the degree of crystallinity of native cellulose using the X-ray diffractometer. Text. Res. J. 1959 ; 29: 786– 794.

[21] Sun, Y.; Cheng, J. J. Hydrolysis of lignocellulosic materials for ethanol production: a review. Bioresource Technology,2002, 83(1), 1–11.

[22] Ahlgren P.A.; Goring D.A.I. Removal of wood components during chlorite delignification of black spruce. Can. J. Chem. 1971, 49, 1272–1275.

[23] Kumar R.; F Huc C.; A Hubbell.; Ragauskas A.J.; Wyman C.E. Comparison of laboratory delignification methods, their selectivity, and impacts on physiochemical characteristics of cellulosic biomass, Bioresour. Technol1. 2013,30, 372–381

[24] Inanaga S.; Okasaka A.; Tanaka S. Does silicon exist in association with organic compounds in rice plants? Soil Sci. Plant Nutr. 1995,41,111-117.

[25] Saito T.; Hirota M.; Tamura N.; Kimura S.; Fukuzumi H.; Heux L.; Isogai A.; Individualization of Nano-Sized Plant Cellulose Fibrils by Direct Surface Carboxylation Using TEMPO Catalyst under Neutral Conditions, Biomacromolecules 2009, 10: 1992–1996

[26] Chaker A.; Alila S.; Mutjé P.; Rei Vilar M.; Boufi S. Effect of the Hemicellulose Content on the Nanofibrillation behaviour of Cellulose Pulps. Cellulose 2013;20:2863-2875.

[27] Tejado A.; Nur Alam M.; Antal M.; Yang H.; van de Ven T.G.M.; Energy requirements for the disintegration of cellulose fibres into cellulose nanofibre. Cellulose 2012,19, 831–842.

[28] Spence K.L.; Venditti R.A.; Rojas O.J.; Habibi Y.; Pawlak J.J. A comparative study of energy consumption and physical properties of microfibrillated cellulose produced by different processing methods, Cellulose 2011, 18,1097–1111

[29] Shibata I.; Isogai A. Depolymerization of cellouronic acid during TEMPO-mediated oxidation. Cellulose, 2003,10, 151-158.

[30] Benhamou K.; Dufresne A.; Magnin A.; Mortha G.; Kaddami H. Control of size and viscoelastic properties of nanofibrillated cellulose from palm tree by varying the TEMPO-mediated oxidation. Carbohyd. Polym. 2014, 99, 74-83.

[31] Favier V. Chanzy H. Cavaille J. Y. Polymer Nanocomposites Reinforced by Cellulose Whiskers

Macromolecules, 1995 ;28 : 6365–6367

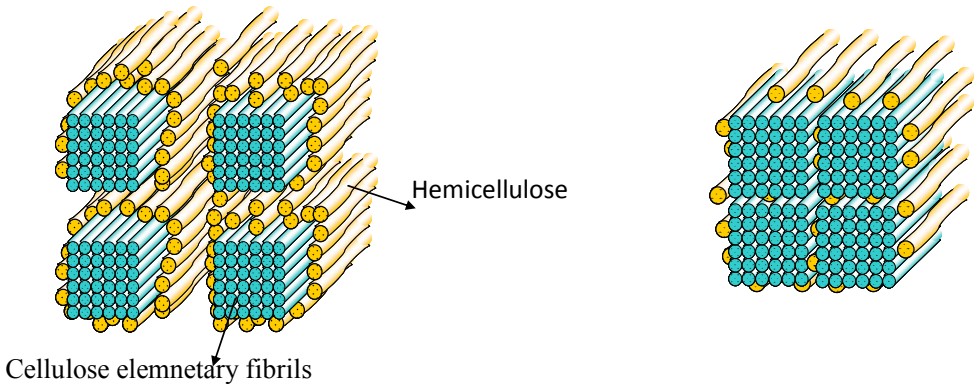

Scheme 2: Schematic illustration of the microfibrils assembly according to the content of hemicellulose within the fibers

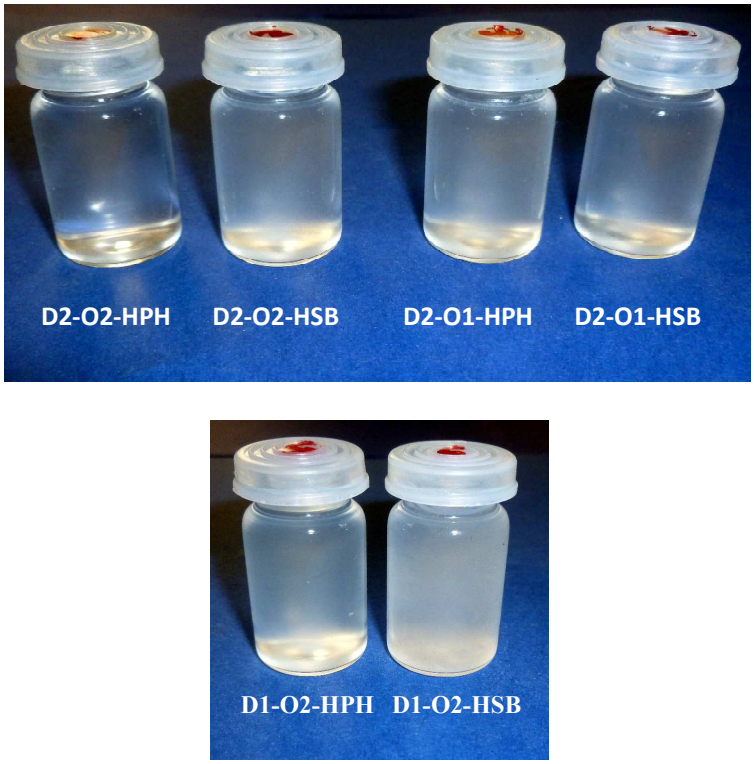

Figure 4: visual aspect of NFC from triticale at a solid content of 1wt%, according to the production mode.

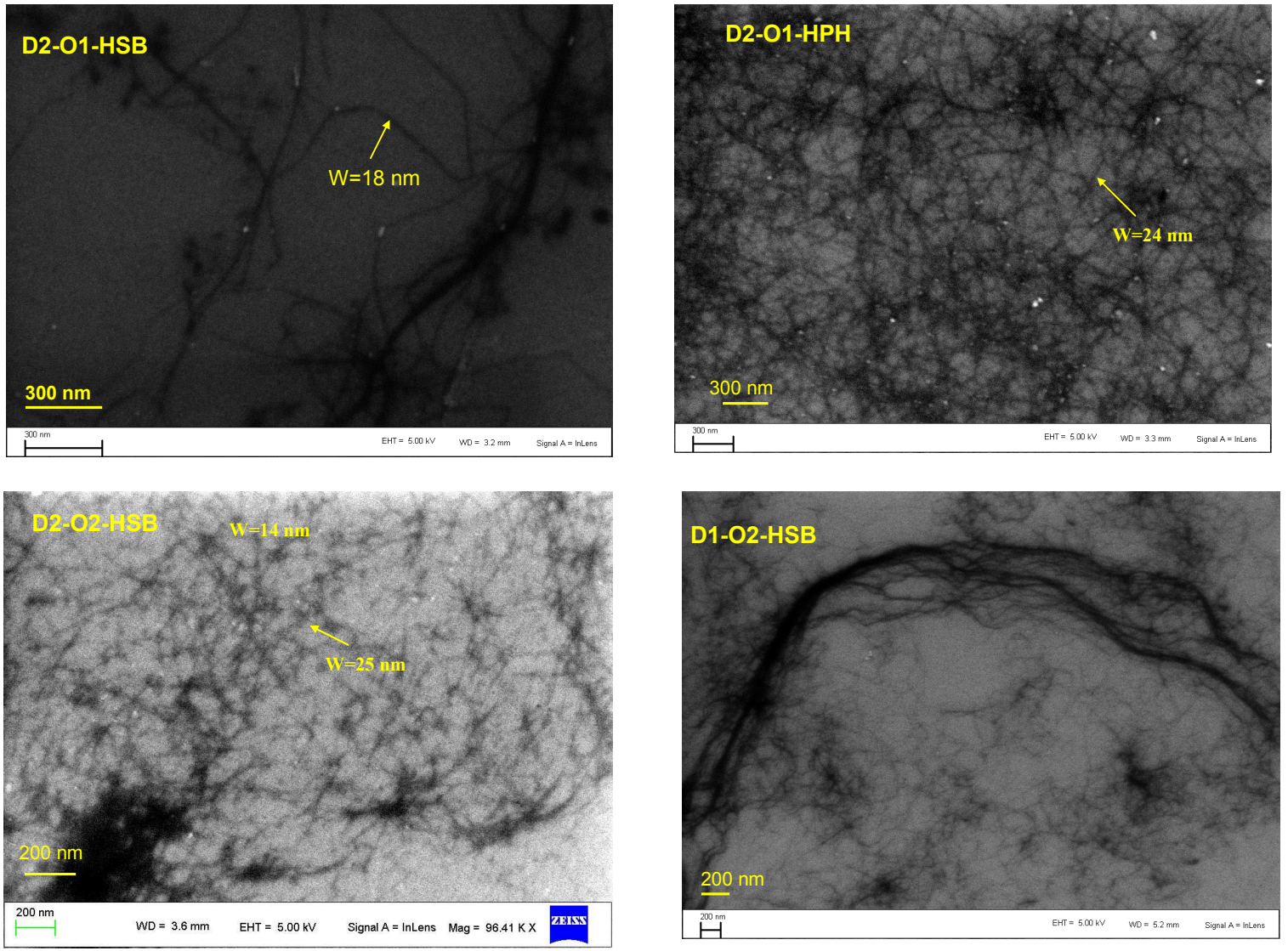

Figure 5: FE-SEM images of NFC produced from tritical straw via high pressure homogenization and high speed blender